# Nonperturbative theory of type-II superconductivity in the presence of a strong Pauli paramagnetic effect

V. Zhuravlev and T. Maniv
*Schulich Faculty of Chemistry, Technion-Israel Institute of Technology, Haifa 32000, Israel*
(Received 8 July 2009; revised manuscript received 12 October 2009; published 19 November 2009)

The unusual low-temperature superconducting (SC) phase transitions following the competition between orbital and spin electron pair breaking, characterizing clean, heavy fermion, strongly type-II superconductors at high magnetic fields, are investigated within a nonperturbaive approach, which enables one to reliably determine the stable SC phases, treat properly the corresponding finite jumps of the order parameter, and account for various unusual features reported recently for some heavy-fermion superconductors such as $CeCoIn_5$ and $URu_2Si_2$.

DOI: 10.1103/PhysRevB.80.174520 PACS number(s): 74.20.−z, 74.25.Bt, 74.81.−g, 74.70.Tx

## I. INTRODUCTION

The phase transition from the superconducting (SC) state to the normal state in strongly type-II superconductors is usually dominated by the orbital (diamagnetic) pair-breaking mechanism due to the characteristically small values of the upper critical field $H_{c2}$ as compared to those of the Pauli paramagnetic limiting field $H_p$.[1] In some heavy-fermion superconductors, however, where the electronic effective masses are sufficiently larger than the free-electron mass and the cyclotron radii at the Fermi surface (FS) are relatively small (see, e.g., Refs. 2 and 3), Pauli paramagnetic pair breaking can dominate the diamagnetic pair-breaking mechanism, and might generate exotic effects such as discontinuous SC phase transitions,[4,5] and spatially modulated SC order parameters along the magnetic field direction.[6,7] A common description of these remarkable phenomena usually exploits a perturbative Ginzburg-Landau (GL) approach[8–12] to qualitatively account for the main features of the corresponding phase diagrams.

Within such a perturbative approach it has been found recently[13] by employing a model of strongly type-II superconductor with a Fulde-Ferrel (FF) modulation of the SC order parameter[6] that in the clean limit the nature of the SC phase transitions depends on the dimensionality of the underlying electronic band structure. For a layered system with the magnetic field direction perpendicular to the layers, a changeover to first-order phase transition can take place in the quasi-two-dimensional (quasi-2D) regime below a critical value of a three-dimensional (3D)-2D crossover parameter. In the 3D limit the normal-to-SC phase transitions are of second order, with the SC phase spatially modulated along the field direction. However, a second transition line from the nonuniform to a uniform SC phase was predicted to be of first order and very close to the normal-to-SC transition line.

The predicted situation for quasi-2D systems below the critical value of the dimensionality parameter, outlined above, seems to account for the changeover of the second-order SC phase transition to a first-order transition, observed recently in specific heat,[14] NMR,[15] and magnetization[16] measurements performed on the heavy-fermion compound $CeCoIn_5$.

Above the critical value of the dimensionality parameter the theory may be applied to the heavy-fermion superconductor $URu_2Si_2$ (whose Fermi surface may be characterized approximately as spherical[3]). In this material a sharp rise of the thermal conductivity with the decreasing magnetic field just below $H_{c2}$ at low temperatures was reported very recently,[17] indicating the existence of a jump in its electronic entropy associated with a first-order phase transition. The theoretically predicted narrow-field interval between the two consecutive phase transitions[13] may account for the observed (smeared) single steplike structure.

In attempting to account for these observations quantitatively a nonperturbative approach with respect to the SC order parameter should be taken since at the discontinuous transitions the order parameter jumps abruptly to finite values. Moreover, as we shall show below, the perturbation theory fails qualitatively in predicting existence of a modulated SC (FF) phase for quasi-2D superconductors.

Thus, we present in this paper a nonperturbative approach to the paramagnetically limited SC phase transitions within the Gorkov's Green's function formalism for a strong magnetic field and low temperature in the lowest Landau-level (LLL) approximation of the Cooper-pair condensate. For the sake of simplicity we will consider only an *s* wave, singlet superconductor, and do not develop further the calculation based on *d*-wave electron pairing presented in Ref. 13. This can be justified in spite of the fact that some of the prominent materials exhibiting strong paramagnetic limiting behavior, such as $CeCoIn_5$, are believed to be unconventional (e.g., *d*-wave) superconductors, which in the presence of nonmagnetic impurities, show qualitatively different $(T,H)$ phase diagrams from those characterizing conventional (*s*-wave) superconductors.[9] However, in the ultraclean limit of interest in the present paper, it was shown in Ref. 13 that the interplay between spin and orbital pair breaking is nearly independent of the type of the electron pairing.

The rest of the paper is organized as follows. The formulation of the physical models under study within the Gorkov's thermodynamic potential scheme is presented in the next section. Critical failures of the common perturbative GL approaches and their corrections by the nonperturbative approach are discussed. Applications to the calculations of the true phase diagrams derived within the nonperturbative theory are presented in Sec. III. In Sec. IV we compare our results with experimental data and discuss their broader implications.

 

## II. THERMODYNAMIC POTENTIAL

### A. Gorkov's perturbation expansion in the SC order parameter

We consider two models of electronic systems which undergo phase transitions to strongly type II, paramagnetically limited superconductivity, under high magnetic fields at low temperatures with a simple zero-field energy dispersion: (1) an isotropic 3D system with $\varepsilon_{\mathbf{k},k_z}^{(3D)}=\frac{\hbar^2|\mathbf{k}|^2}{2m_\perp^*}+\frac{\hbar^2k_z^2}{2m_z}$, $m_z=m_\perp^*$, where $\mathbf{k}=\hat{\mathbf{x}}k_x+\hat{\mathbf{y}}k_y$ and (2) a quasi-2D system with $\varepsilon_{\mathbf{k},k_z}^{(q2D)}=\frac{\hbar^2|\mathbf{k}|^2}{2m_\perp^*}+t_z[1-\cos(k_zc)]$, where $t_z$ is the interlayer transfer integral and $c$ is the interlayer distance. The external magnetic field, $\mathbf{H}=H\hat{z}$, is perpendicular to the easy conducting $(xy)$-plane in the quasi-2D model where the energy spectrum experiences Landau quantization. The first model may be relevant for the SC phase transitions in $URu_2Si_2$, while the second model can be applied to the SC transitions in $CeCoIn_5$.

We start the formal part of the paper by writing an expansion of the grand thermodynamic potential (TP), $\Omega$, in the SC order parameter, $\Delta(\mathbf{r})$, using BCS theory for the usual singlet $s$-wave electron pairing, as presented recently in Ref. 13. Thus we write

$$\Omega(\Delta_0)=V\frac{\Delta_0^2}{(\hbar\omega_c)^2g_{int}}+\sum_{n=1}\frac{(-1)^n}{n}\Omega_{2n}(\Delta_0),$$

$$\Omega_{2n}=\int d^3\{\mathbf{r}\}\Gamma_{2n}(\{\mathbf{r}\},\Delta_0)K_{2n}(\{\mathbf{r}\}), \tag{1}$$

where $g_{int}$ is the effective BCS coupling constant, $V$ is the volume

$$\Gamma_{2n}(\{\mathbf{r}\},\Delta_0)=g^*(\mathbf{r}_1,\mathbf{r}_2)g(\mathbf{r}_2,\mathbf{r}_3)\ldots g^*(\mathbf{r}_{2n-1},\mathbf{r}_{2n})g(\mathbf{r}_{2n},\mathbf{r}_1)\Delta(\mathbf{r}_1)\Delta^*(\mathbf{r}_2)\ldots\Delta(\mathbf{r}_{2n-1})\Delta^*(\mathbf{r}_{2n}) \tag{2}$$

and

$$K_{2n}(\{\mathbf{r}\})=k_BT\sum_\nu\hat{G}_{0\downarrow}^*(\mathbf{r}_1,\mathbf{r}_2,\omega_\nu)\hat{G}_{0\uparrow}(\mathbf{r}_2,\mathbf{r}_3,\omega_\nu)\ldots\hat{G}_{0\downarrow}^*(\mathbf{r}_{2n-1},\mathbf{r}_{2n},\omega_\nu)\hat{G}_{0\uparrow}(\mathbf{r}_{2n},\mathbf{r}_1,\omega_\nu). \tag{3}$$

Here $\Delta_0^2=V^{-1}\int d^3\mathbf{r}_i|\Delta(\mathbf{r}_i)|^2$ is the spatially averaged squared order parameter, and $\{\mathbf{r}\}=\{\mathbf{r}_1,\ldots,\mathbf{r}_{2n}\}$ denotes the entire set of position vectors for a cluster consisting of $n$ electron pairs. Note that for convenience we incorporated the gauge factors, $g(\mathbf{r}_i,\mathbf{r}_{i+1})$, of the Green's functions, $G_{0\downarrow}(\mathbf{r}_i,\mathbf{r}_{i+1},\omega_\nu)$, for a free electron in a uniform magnetic field, into the vertex part, $\Gamma_{2n}$, so that the effective kernel $K_{2n}$ is given in Eq. (3) by a product of the gauge invariant Green's functions, $\hat{G}_{0\uparrow\downarrow}(\mathbf{r}_i,\mathbf{r}_{i+1},\omega_\nu)$. A useful expression for such a Green's function for a positive Matsubara frequency, $\nu\geq0$, can be written as (see Appendix A)

$$i\hat{G}_{0\uparrow\downarrow}(\mathbf{r}_1,\mathbf{r}_2,\omega_\nu)=\frac{1}{2\pi a_H^3\hbar\omega_c}\int\frac{dk_z}{2\pi}e^{ik_z(z_2-z_1)}e^{-\rho_{12}^2/4}\times\int_0^\infty d\tau e^{i\tau[n_F+g-\varepsilon_z(k_z)/\hbar\omega_c+i\varpi_\nu]}\times(1-e^{-i\tau})^{-1}\exp\left(-\frac{\rho_{12}^2e^{-i\tau}}{2(1-e^{-i\tau})}\right), \tag{4}$$

where $\rho_{1,2}\equiv\mathbf{r}_{\perp2}-\mathbf{r}_{\perp1}$, with $\mathbf{r}_{\perp1}$ and $\mathbf{r}_{\perp2}$ the projections of the initial and final electron position vectors, respectively, on the $(x$-$y)$ plane perpendicular to the magnetic field. This expression is obtained after summation over the LL index $n=0,1,\ldots$ of the single electron energy, $\varepsilon_{n,k_z}^{\uparrow\downarrow}/\hbar\omega_c=n+\varepsilon_z(k_z)/\hbar\omega_c\mp g-n_F+i\varpi_\nu$ for a spin up (or down), with the in-plane cyclotron frequency $\omega_c=eH/m_\perp^*c$, Zeeman spin energy $\mp eH/m_0c$, and $g$ factor $g\equiv m_\perp^*/m_0$, with $m_\perp^*$, $m_0$—the in-plane effective mass and the free-electron mass, respectively. Here $n_F=\mu/\hbar\omega_c-1/2$, $\mu$—the Fermi energy, and $\varpi_\nu=\omega_\nu/\omega_c$, with $\omega_\nu=(2\nu+1)\pi k_BT/\hbar$, the Matsubara frequency. Space coordinates and momenta are expressed in units of $a_H$ and $a_H^{-1}$, respectively, where $a_H=\sqrt{c\hbar/eH}$ is the magnetic length. The electronic energy along the field direction, $\varepsilon_z^{(3D)}=\frac{\hbar^2k_z^2}{2m_z^*}$ for the isotropic 3D case and $\varepsilon_z^{(q2D)}=t_z[1-\cos(k_zc)]$ for the quasi-2D one, is denoted by $\varepsilon_z(k_z)$. In the former case the integral over $k_z$ is performed in the entire free-electron range: $-\infty<k_z<\infty$, whereas in the latter it is carried out within the first Brillouin zone (BZ): $-\frac{\pi}{c}<k_z<\frac{\pi}{c}$.

For the sake of simplicity, we consider only a single-mode (FF) modulation of the order parameter.[6] Multimode modulation such as in the Larkin-Ovchinnikov (LO) state,[7] which may be important at low temperatures,[9,10] is not expected to drastically change our main conclusions (see a discussion below). Thus, the SC order parameter is assumed to take the form, $\Delta(\mathbf{r},z)=\Delta_{\max}e^{iqz}\varphi_0(x,y)$, where $\Delta_{\max}^2=(\frac{2\pi}{a_x^2})^{1/2}\Delta_0^2$, and $\varphi_0(x,y)$ describes (in the symmetric gauge) a rectangular vortex lattice with intervortex distance, $a_x$

$$\varphi_0(x,y)=e^{ixy}\sum_k e^{iq_kx-(y-q_k/2)^2}=e^{-1/2|u|^2+1/2u^2}\sum_k e^{iq_kz-q_k^4/4}$$

while $e^{iqz}$ is a FF modulation function along the magnetic field direction, controlled by the wave number, $q$. Here $q_k=2\pi k/a_x$, and $u=x+iy$ is a complex coordinate in the plane perpendicular to magnetic field. Note that the exact form of the vortex lattice is irrelevant in the present problem.

### B. The vertex part in the local approximation

The vertex part $\Gamma_{2n}(\{\mathbf{r}\},\Delta_0)$, Eq. (2), is a violently oscillating function of the lateral relative electronic coordinates $\rho_{i,i+1}\equiv \mathbf{r}_{\perp i+1}-\mathbf{r}_{\perp i}$, $i=1,2,\ldots,2n$, $\mathbf{r}_{\perp 2n+1}=\mathbf{r}_{\perp 1}$, which interferes strongly with the oscillatory electronic kernel $K_{2n}(\{\mathbf{r}\})$, Eq. (3). Multiple integration over these coordinates yields gross cancellations except near stationary configurations, which restrict all $2n$ electronic position vectors to a relative proximity region of size of a magnetic length.[18,19] Other contributions to this integral, arising from nonstationary, separately paired configurations, such as: $\boldsymbol{r}_{\perp 1}=\boldsymbol{r}_{\perp 2}$, $\boldsymbol{r}_{\perp 3}=\boldsymbol{r}_{\perp 4}$ and $\boldsymbol{r}_{\perp 1}=\boldsymbol{r}_{\perp 4}$, $\boldsymbol{r}_{\perp 3}=\boldsymbol{r}_{\perp 2}$, in the case of the quartic term ($n=2$), become increasingly important with the increasing order, $n$, of the expansion. However, since the self-consistent (mean-field) value of the order parameter is restricted to relatively small values, nonlocal contributions to the nonoscillatory component[18,19] of the TP may be neglected to any significant order in the expansion, and the vertex part may be written in the simple form

$$\Gamma_{2n}(\{\mathbf{r}\},\Delta_{\max}) = \Delta_{\max}^{2n} e^{-1/2\Sigma_i|u_i|^2+1/2(u_1^2+u_2^{*2}+\cdots+u_{2n-1}^2+u_{2n}^{*2})}\frac{a_x}{2\pi}\int dq_0 e^{-nq_0^2/2+iq_0(u_1-u_2^*\ldots-u_{2n}^*)}e^{iq(z_1-z_2\ldots-z_{2n})}$$

$$\simeq \frac{a_x\sqrt{\pi}}{2\pi}\frac{2}{\sqrt{2n}}\Delta_{\max}^{2n}e^{iq(z_1-z_2\ldots-z_{2n})}e^{-1/4\Sigma\boldsymbol{\rho}_{i,i+1}^2}, \tag{5}$$

in which all off-diagonal terms involving different Landau orbitals are neglected. Here an *ad hoc* notation for the spatial coordinates, $u_k=x_k+iy_k$, has been used. This additional simplification is justified since the off-diagonal terms, which are sensitive to the vortex lattice structure, are proportional to the small Gaussian factors, $\exp[-(\pi^2/a_x^2)\Sigma_{j,l=1}^{n}(k_{2j}-k_{2l-1})^2]$, with the orbital quantum numbers $k_j$ $(j=1,\ldots,2n)$ obeying the conservation law: $\Sigma_{j=1}^{2n}(-1)^j k_j=0$. This property is closely related to the weak dependence of the SC condensation energy on the vortex lattice structure.[19,20] Consequently, the remaining sum of the dominant diagonal terms is approximated in Eq. (5) by an integral (over $q_0$). The great advantage of using Eq. (5) in Eq. (1) is in its factorization with respect to the relative coordinate and its apparent independence of the center-of-mass coordinate, which enable us rewriting the integrand in Eq. (1) as a separable product of "new" single electron Green's functions, $e^{-1/4\boldsymbol{\rho}_{i,i+1}^2}\hat{G}_{0\uparrow\downarrow}(\rho_{i,i+1}^2,\omega_\nu)$.

### C. Summation of the perturbation series

The corresponding $n$th order term, $\Omega_{2n}$, can be thus written as a 3D integral over the center of mass momentum of an effective two-particle Green's function, raised to the $n$th power, by performing an appropriate Fourier transformation (see Appendix B), that is

$$\Omega_{2n}(\Delta_{\max}) = V\frac{k_BT}{a_H^3}\frac{a_x}{\sqrt{2\pi n}}\tilde{\Delta}_{\max}^{2n}I_{2n}, \tag{6}$$

where $\tilde{\Delta}_{\max}=\frac{\Delta_{\max}}{\hbar\omega_c}$, and

$$I_{2n} = \sum_{\nu>0}\int\frac{d^2kdk_z}{(2\pi)^3}[\tilde{\Phi}_\nu(\mathbf{k},k_z|g,q)\tilde{\Phi}_\nu^*(\mathbf{k},k_z|-g,-q)]^n + \text{c.c.}, \tag{7}$$

$$\tilde{\Phi}_\nu(\mathbf{k},k_z|g,q) = \int_0^\infty d\tau e^{-\tau[\varpi_\nu+i\tilde{\xi}_{\mathbf{k},k_z}(g,q)]-1/2(1-i\tau-e^{-i\tau})|\mathbf{k}|^2},$$

$$\tilde{\xi}_{\mathbf{k},k_z}(g,q) = \frac{1}{2}|\mathbf{k}|^2 + \frac{\varepsilon_z(k_z-q/2)}{\hbar\omega_c} - g - n_F, \quad \mathbf{k}=\hat{\mathbf{x}}k_x+\hat{\mathbf{y}}k_y. \tag{8}$$

Note that in these expressions and in what follows a tilde above a symbol indicates that it is calculated with energy measured in units of $\hbar\omega_c$. The resulting perturbation series can be easily summed to all orders, provided the reduction prefactor $\frac{1}{\sqrt{n}}$, arising from the overlap integral of $n$ LLL orbitals in Eq. (5), is represented as a Gaussian integral: $\frac{2}{\sqrt{\pi}}\int_0^\infty \exp(-nu^2)du$, with the result

$$\frac{\Omega}{V} = \frac{a_x}{\sqrt{2\pi}}\left[\frac{\tilde{\Delta}_{\max}^2}{g_{int}} - \frac{k_BT}{a_H^3}\mathrm{Re}\sum_{\nu>0}\left\langle\int\frac{d^3k}{(2\pi)^3}\times\ln(1+e^{-u^2}\tilde{\Delta}_{\max}^2\tilde{\Theta}_\nu)\right\rangle_u\right], \tag{9}$$

$$\tilde{\Theta}_\nu = \tilde{\Phi}_\nu(\mathbf{k},k_z|g,q)\tilde{\Phi}_\nu^*(\mathbf{k},k_z|-g,-q), \tag{10}$$

where $\langle f(u)\rangle_u\equiv\frac{2}{\sqrt{\pi}}\int_0^\infty duf(u)$. Note the prefactor $a_x/\sqrt{2\pi}$ ($\approx 0.76$ for the hexagonal lattice) in Eq. (9), which takes into account the reduction in the SC free energy associated with the vortex core regions, and the maximal value of the SC order parameter, $\tilde{\Delta}_{\max}$, in the vortex lattice unit cell.

The self-consistency equation for the order parameter, obtained from the variational condition $\tilde{\Delta}_{\max}^2\frac{\partial}{\partial\tilde{\Delta}_{\max}^2}(\frac{\Omega}{V})=0$, is written as

$$\frac{\tilde{\Delta}_{\max}^2}{g_{int}} = \frac{k_B T}{a_H^3} \int \frac{d^3k}{(2\pi)^3} \mathrm{Re} \sum_{\nu>0} \left\langle \frac{e^{-u^2} \tilde{\Delta}_{\max}^2 \tilde{\Theta}_\nu}{1 + e^{-u^2} \tilde{\Delta}_{\max}^2 \tilde{\Theta}_\nu} \right\rangle_u . \quad (11)$$

A simple limiting situation for testing this nonperturbative result in the zero magnetic field limit was solved exactly long time ago by Gorkov (see, e.g., Ref. 21). For $H \to 0$ the integrand in Eq. (8) ($\sim e^{-1/2(1-i\tau-e^{-i\tau})|\mathbf{k}|^2}$, with $|\mathbf{k}|$ measured in $a_H^{-1}$ units) is negligible except for very small $\tau$ values, for which $\frac{1}{2}(1-i\tau-e^{-i\tau})|\mathbf{k}|^2 \to \frac{1}{4}\tau^2|\mathbf{k}|^2 \ll \tau\varpi_\nu$, so that the integral over $\tau$ yields the free-electron Green's function: $\frac{i}{i\varpi_\nu - \xi_{\mathbf{k},k_z}}$. The resulting expression on the RHS of Eq. (11) is similar to that obtained in Ref. 21 at zero magnetic field, except for the averaging over $u$, which takes into account the constraint imposed on the electrons to be in the LLL in our high-field approach.

Another limiting case is the quasiclassical limit ($\frac{E_F}{\hbar\omega_c} \gg 1$, $\frac{2\pi^2 k_B T}{\hbar\omega_c} \gtrsim 1$) of a BCS superconductor in a magnetic field with a uniform ($q=0$) SC order parameter along the field direction, without spin splitting ($g=0$). Here the dominant contribution to the effective two-particle Green's function, Eq. (8), originates in the integration region $\tau \ll 1$ so that $e^{i\tau}$ can be expanded up to second order to yield the Gaussian approximation

$$\tilde{\Phi}_\nu(\mathbf{k},k_z|g,q) \approx \int_0^\infty d\tau e^{-\tau[\varpi_\nu + i\xi_{\mathbf{k},k_z}(g,q)] - 1/4\tau^2|\mathbf{k}|^2}, \quad (12)$$

in which quantum magnetic oscillations and other quantum corrections are neglected. Expansion of the RHS of Eq. (11) up to first order in $e^{-u^2}\tilde{\Delta}_{\max}^2\tilde{\Theta}_\nu$ yields the well-known Helfand-Werthamer self-consistency equation for $H_{c2}(T)$.[22]

### D. Rescaled expression for the thermodynamic potential

In what follows it will be convenient to employ field-independent normalization for the order parameter and related quantities by changing the energy scale $\hbar\omega_c$ to $\pi k_B T_{c0}$, with $T_{c0}$ the transition temperature at zero magnetic field, and the corresponding length scale $a_H$ to $\xi \equiv \sqrt{\frac{\hbar^2}{2m_\perp^* \pi k_B T_{c0}}}$. The latter length is related to the in-plane BCS coherence length, $\xi(0) = \frac{0.18\hbar v_F}{k_B T_{c0}}$, where $v_F \equiv \hbar k_F / m_\perp^*$ and $k_F \equiv \sqrt{2m_\perp^* \mu/\hbar^2}$, via $\xi = \frac{0.94}{\sqrt{k_F \xi(0)}}\xi(0)$.

In terms of the rescaled parameters Eq. (9) takes the form

$$\frac{\Omega}{V\Xi_0} = \alpha_{int}\bar{\Delta}_{\max}^2 - \frac{(2\pi)^2 t}{\pi\sqrt{\bar{\mu}}} \mathrm{Re} \sum_{\nu>0} \left\langle \int \frac{d^3k}{(2\pi)^3} \times \ln(1 + \bar{\Delta}_{\max}^2 e^{-u^2}\bar{\Theta}_\nu) \right\rangle_u , \quad (13)$$

where $t \equiv T/T_{c0}$, and

$$\bar{\Theta}_\nu = \bar{\Phi}_\nu(\mathbf{k},k_z|g,q)\bar{\Phi}_\nu^*(\mathbf{k},k_z|-g,-q), \quad \bar{\Delta}_{\max}^2 = \frac{\Delta_{\max}^2}{(\pi k_B T_{c0})^2}.$$

Note that in these expressions and in what follows a bar above a symbol indicates that it is calculated with energy measured in units of $\pi k_B T_{c0}$. Since we use $T_{c0}$ as an input parameter, the coupling constant, $\alpha_{int}$, is determined here from the self-consistency Eq. (11) at $\Delta_{\max}=0$ and $H=0$, i.e.,

$$\alpha_{int} = \frac{(2\pi)^2}{\pi\sqrt{\bar{\mu}}} \sum_{\nu>0} \int \frac{d^3k}{(2\pi)^3} \frac{1}{(2\nu+1)^2 + [k^2 + \bar{\varepsilon}_z(k_z) - \bar{\mu}]^2}.$$

Exploiting the quasiclassical (Gaussian) approximation, Eq. (12), the effective Green's function, $\bar{\Phi}_\nu$, can be reduced to

$$\bar{\Phi}_\nu(\mathbf{k},k_z|g,q) \simeq \int_0^\infty d\tau e^{-\tau[t(2\nu+1) + i\bar{\xi}_{\mathbf{k},k_z}(g,q)] - bk^2\tau^2/2\eta^2\bar{\mu}} = \frac{w(x_\nu)}{(2\nu+1)t + i\bar{\xi}_{\mathbf{k},k_z}}, \quad (14)$$

where $w(x) = \sqrt{\pi} x e^{x^2} Erfc(x)$, with $x_\nu = \eta \frac{\sqrt{\bar{\mu}}[(2\nu+1)t + i\bar{\xi}_{\mathbf{k},k_z}]}{\sqrt{2bk}}$ and the renormalized single electron energy: $\bar{\xi}_{\mathbf{k},k_z}(g,q) = k^2 + \bar{\varepsilon}_z(k_z - q/2) - \bar{g}b - \bar{\mu}$, $b \equiv \frac{H}{H_{c20}}$. The renormalized parameters are defined as $\bar{\mu} = \frac{\mu}{\pi k_B T_{c0}}$, $\bar{g} = g\frac{\hbar\omega_{c20}}{\pi k_B T_{c0}}$, $\bar{\varepsilon}_z = \frac{\varepsilon_z}{\pi k_B T_{c0}}$, and $\Xi_0 = \frac{a_x}{\sqrt{2\pi}} \frac{\sqrt{k_B T_{c0}\mu}}{2\pi\xi^3}$. The quantity

$$\eta = \frac{\pi k_B T_{c0}}{\sqrt{\hbar\omega_{c20}\mu}}, \quad (15)$$

with $\omega_{c20} = eH_{c20}/m_\perp^* c$, is a constant of the order unity relating the transition temperature at zero field, $T_{c0}$, to the upper critical field, $H_{c20}$, at zero temperature for $g=0$ and $q=0$. For the BCS-like theory employed here this constant defines a single scaling function determining the entire $H$-$T$ phase boundary in the absence of the Pauli paramagnetic effect. Its numerical value depends on the material electronic band structure, e.g., on the interlayer tunneling integral $t_z$ in the present model (see below) and on the type of electron pairing.

### E. Diamagnetic versus Pauli paramagnetic effect

Equation (14) provides us with a simple expression for the diamagnetic effect on the single-electron propagator involved in paramagnetically limited pairing. It consists of the usual Green's function in momentum space for an electron in the presence the Zeeman (paramagnetic) spin splitting and a correction factor, due to the orbital (diamagnetic) effect, expressed by the function $w(x_\nu)$. The latter function varies between the asymptotic value $w(x_\nu) \to 1$ at large $|x_\nu|$, which reflects the limit of no diamagnetic effect (e.g., for $b \ll 1$), and the limiting value $w(x_\nu) \to \sqrt{\pi} x_\nu \propto (2\nu+1)t + i\bar{\xi}_{\mathbf{k},k_z}$ at small $|x_\nu|$, which strongly modifies the Green's function due to diamagnetic effects (see Fig. 1). The strong variation in the complex function $w(x)$ around the origin, shown in Fig. 1, reflects the restriction of the diamagnetic effects appearing at high fields and low temperatures to electrons with energies close to the Fermi energy.

To gain further insight into the structure of Eq. (13) let us consider the two-particle distribution function, $D(|\mathbf{k}|) = \frac{t}{\pi\sqrt{\bar{\mu}}}|\mathbf{k}| \mathrm{Re} \int dk_z \Theta_{\nu=0}(\mathbf{k},k_z)$, in momentum space perpendicular to the magnetic field (see Fig. 2). The sharp peak at $|\mathbf{k}|$

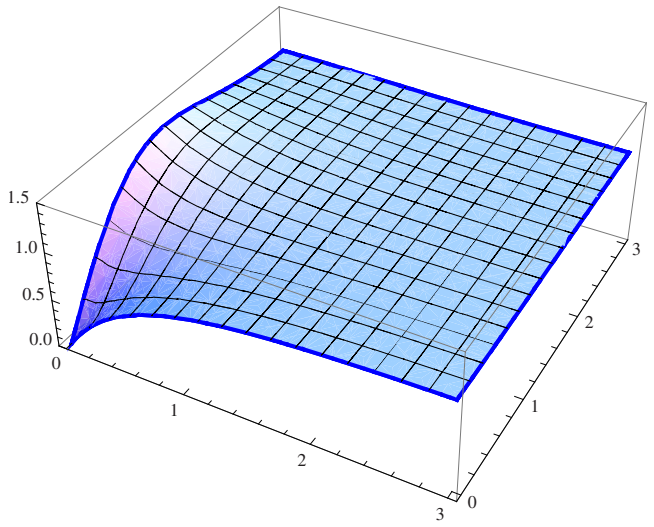


FIG. 1. (Color online) The modulus of $w(x_\nu)$ in the complex $x_\nu$ plane. Note that $|w(x_\nu)|$ deviates significantly from unity only around the origin where $|x_\nu| \lesssim 1$.

$\sim k_F$, shown in Fig. 2, for a system without spin splitting, $\bar{g}=0$, reflects an enhancement of the contribution to the SC condensation energy from electrons around the extremal Landau orbit, $n \sim n_F = \tilde{\mu}$, $k_z \sim 0$. However, the overall contribution to pairing from electrons away from this region, $n < n_F$, $k_z \sim k_F = \sqrt{\tilde{\mu}}$, is still significant. Strong spin splitting, e.g., at $\bar{g}=3$, reduces the pairing energy for the uniform state $q=0$ in the entire electron spectrum, leading to a stronger localization around the extremal Landau orbit. For electron pairs with nonzero small $q$ this localization effect is significantly weakened but recovered for larger $q$ (see Fig. 2).

The quasiclassical expression for the Green's function, Eq. (14), has been used in the numerical calculations presented in the next sections. However, for illustrating the main qualitative features of the diamagnetic effect, it is instructive to use an approximate simple expression for the function $\bar{\Phi}_\nu(\mathbf{k}, k_z | g, q)$ by exploiting a "relaxation time" (RT) approximation, $e^{-\pi/\tau_0(|\mathbf{k}|)}$, for the Gaussian factor, $e^{-bk^2\tau^2/2\eta^2\bar{\mu}}$, appearing in Eq. (12), with a relaxation time $\tau_0(|\mathbf{k}|) \equiv \sqrt{\frac{2\eta^2\bar{\mu}}{bk^2}}$. The corresponding effective single-particle Green's function, Eq. (12), takes a familiar form

$$\bar{\Phi}_\nu^{(RTA)}(\mathbf{k}, k_z | g, q) = \frac{1}{(2\nu+1)t + \tau_0^{-1}(|\mathbf{k}|) + i\xi_{\mathbf{k},k_z}(g,q)} \tag{16}$$

with $\tau_0^{-1}(|\mathbf{k}|) \sim b^{1/2}|\mathbf{k}|$ determining a rate of diamagnetic "pair relaxation" in addition to the usual rate of thermal pair breaking. Equation (16) explicitly shows that the diamagnetic effect is important for quasiparticles with sufficiently large momentum components in the plane perpendicular to the magnetic field, satisfying $b^{1/2}|\mathbf{k}| \gtrsim tk_F$.

The reliability of this approximation can be examined by comparing the numerically calculated distribution function, $D(|\mathbf{k}|)$ with that obtained in the RT approximation (see Fig. 2), which can be readily evaluated analytically for a 3D system. For a nonzero spin splitting $D^{(RTA)}(|\mathbf{k}|)$ has a form similar to $D(|\mathbf{k}|)$ at the same spin-splitting parameter, so that most of the results obtained within the RT approximation are qualitatively correct. Nevertheless, some important fine features, such as the dependence of the phase diagram on dimensionality, may not be correctly described in this simplified framework.

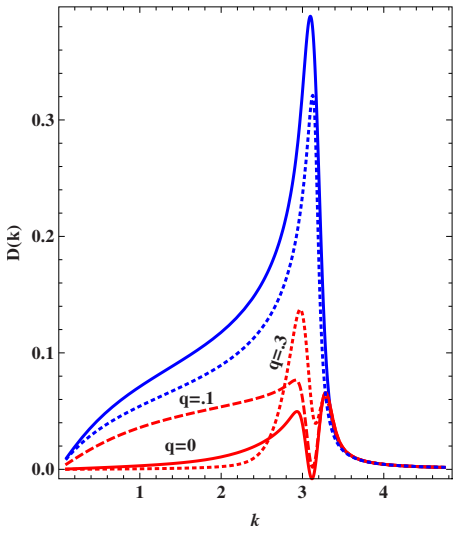


FIG. 2. (Color online) The pair-distribution function $D(|\mathbf{k}|)$, at $t=0.1$ and $b=0.2$, for an isotropic 3D metal with $\bar{g}=0$ (two upper curves) and $\bar{g}=3$ (three lower curves) for different modulation wave numbers along the $z$ axis: $q=0$ (solid), $q=0.1$ (dashed), and $q=0.3$ (dotted). The upper (blue) dotted line represents the RT approximation for $\bar{g}=0$.

### F. Failures of the low-order perturbation theory

In this section we reveal critical failures of the perturbation GL theory used in the existing literature, which entail development of the nonperturbative theory presented in this paper. This is done by expanding the expression for $\Omega(\bar{\Delta}^2_{\max})$, Eq. (13), in power series of $\bar{\Delta}^2_{\max}$, i.e.,

$$\Omega_{pert}/V\Xi_0 = \alpha\bar{\Delta}^2_{\max} + \frac{1}{2}\beta\bar{\Delta}^4_{\max} + \frac{1}{3}\gamma\bar{\Delta}^6_{\max} + \cdots, \tag{17}$$

and comparing to the nonperturbative result. Thus, up to the second order in $\tilde{\Delta}^2_{\max}$, we find that

$$\alpha = \alpha_{int} - \frac{(2\pi)^2 t}{\pi\sqrt{\bar{\mu}}} \sum_{\nu>0} \int \frac{d^3k}{(2\pi)^3} \mathrm{Re}\,\Theta_\nu, \tag{18}$$

$$\beta = \frac{1}{2^{1/2}} \frac{(2\pi)^2 t}{\pi\sqrt{\bar{\mu}}} \sum_{\nu>0} \int \frac{d^3k}{(2\pi)^3} [(\mathrm{Re}\,\Theta_\nu)^2 - (\mathrm{Im}\,\Theta_\nu)^2], \tag{19}$$

which imply that the "ill" behavior of $\Theta_\nu$ in the presence of strong spin splitting, namely, that $\mathrm{Re}\,\Theta_\nu < 0$ and $\mathrm{Im}\,\Theta_\nu \neq 0$, can lead under certain circumstances, within the low-order GL expansion, to a changeover to first-order SC phase transition. Indeed, Eq. (18) shows that $\mathrm{Re}\,\Theta_\nu < 0$ can prevent the critical behavior of $\alpha$ by reversing the sign of the second

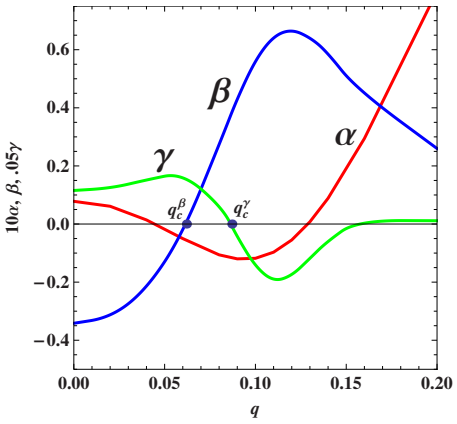


FIG. 3. (Color online) Dependence of the GL coefficients $\alpha$ (red line), $\beta$ (blue line), and $\gamma$ (green line) on the modulation wave number $q$ for an isotropic 3D system with $\bar{g}=1.8$, at $t=0.2$ and $b=0.185$. Note the optimal $q=q_{opt}\simeq .1$, corresponding to a minimal value of $\alpha$, where $\beta$ is positive, resulting in a second-order phase transition from the normal to a nonuniform SC state within low-order perturbation theory.

term on its RHS, whereas from Eq. (19) one concludes that $|\mathrm{Im}\,\Theta_\nu|>|\mathrm{Re}\,\Theta_\nu|$ can lead to $\beta<0$ (see Fig. 3). For a strong spin splitting such anomalous behavior of the coefficient $\beta$ occurs at the second-order "transition" line, $\alpha=0$, below some critical temperature $T^*$. One might expect that the next-order term, with the coefficient $\gamma(q=0)$ being usually positive (see Fig. 3), fixes the second-order perturbation theory and provides a correct result. Under these circumstances the third-order perturbative GL free energy, Eq. (17), yields a first-order SC phase transition at $\Omega(\bar{\Delta}^2_{\max})=0$ with $\bar{\Delta}^2_{\max}=\frac{3|\beta|}{4\gamma}$ and $\alpha=\frac{3\beta^2}{16\gamma}>0$. However, due to very small values of $\gamma(q=0)$, the position of the energy minimum is shifted to a large value of $\bar{\Delta}^2_{\max}(\bar{\Delta}^2_{\max}\approx 0.23)$, where the perturbation theory is not valid. A lower bound on the radius of convergence for both second- and third-order theories can be estimated as $\bar{\Delta}^2_{\max}\lesssim 0.02$.

The application of the perturbation theory to the nonuniform states is even more troublesome since the expansion coefficients oscillate with the modulation wave number $q$ (see Fig. 3). Near the optimal FF wave number $q=q_{opt}$ (e.g., $\approx 0.1$ in Fig. 3), where the second-order perturbation theory (in contrast to the third-order theory) correctly describes the continuous phase transition to the nonuniform (FF) SC state, this oscillatory dependence provides the means for healing the anomalous behavior of the coefficients arising from the strong spin splitting (see, e.g., the anomalous behavior in Fig. 3 near $q=0$ and its healing near $q=q_{opt}$). The reliability of the second-order theory quickly deteriorates away from $q_{opt}$, e.g., in approaching the region $q\approx 0.06-0.08$ in Fig. 3, where both coefficients $\beta$ and $\gamma$ change sign.

The trouble with the standard GL theory of the modulated state is illustrated in Fig. 4 where the minimized TP with respect to $\bar{\Delta}^2_{\max}$, obtained from the nonperturbative approach and from the second-order perturbation expansion, is shown as functions of the modulation parameter $q$. The curve, representing the nonperturbative theory near a first-order transition, has a clear double-well structure corresponding to the uniform and nonuniform SC states. The curve representing the second-order theory shows a divergent free energy at a critical $q_c^\beta$, where $\beta(q_c^\beta)=0$ (see Fig. 3). The removal of this singularity in the third-order theory, due to the positive value of $\gamma$ at $q_c^\beta$, is not very helpful since the latter theory becomes also unreliable in slightly varying $q$ due to the nearby critical point $q_c^\gamma$, where $\gamma(q_c^\gamma)=0$.

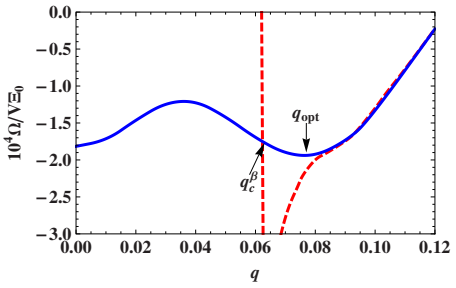


FIG. 4. (Color online) Comparison of the SC free energy, at $t=0.2$ and $b=0.185$, obtained from the nonperturbative approach for an isotropic 3D system as a function of $q$ (solid curve) with the corresponding second-order perturbative result, $-\frac{\alpha^2}{2\beta}$ (dashed curve). The perturbation theory correctly indicates the very existence of a first-order phase transition but fails badly to describe it quantitatively. The material parameters used, $\bar{\mu}=10$, $\bar{g}=1.8$, are characteristic of $URu_2Si_2$.

## III. APPLICATIONS OF THE NONPERTURBATIVE THEORY: PHASE DIAGRAMS

The analysis presented in the preceding section shows that one may not trust the perturbative GL approach even for qualitative purposes, such as schematic determination of the $H$-$T$ phase diagram, needless to say for quantitative applications. In the present section we apply the nonperturbative method developed in Sec. II in determining the phase diagrams for the two electronic models outlined there.

Quantitatively speaking, the most significant effect of the paramagnetic pair breaking on the phase diagram at low temperature $T$ is its dramatic (i.e., by nearly an order of magnitude in typical cases) suppression of $H_{c2}^{(0)}(T)$ as compared to the upper critical field determined solely by the diamagnetic pair breaking. In addition to this effect, which can be estimated within the perturbative GL approach by the usual condition for a second-order phase transition into a uniform SC state, $\alpha(q=0)=0$, there are (much weaker) enhancement mechanisms of $H_{c2}(T)$, which are operative at different temperatures. At temperatures $T$ below $T_{fflo}$, where the curvature $\kappa=\frac{\partial^2}{\partial q^2}\alpha(q=0)$ along the line $\alpha(q=0)=0$ is negative, one expects (within perturbation theory) a second-order phase transition into a modulated state at $H_{c2}^{(2)}$, with an optimal value $q=q_{opt}$ satisfying $\alpha(q=q_{opt})=0$. Thus, for the corresponding uniform state one has: $\alpha(q=0)>0$ (see Fig. 3), implying that $H_{c2}^{(2)}>H_{c2}^{(0)}$. At temperatures $T$ below $T^*$, where $\beta(q=0)$ is negative along the line $\alpha(q=0)=0$, one expects (again within perturbation theory) a first-order phase transition into a uniform SC state for another positive $\alpha(q=0)$ value (given, e.g.,

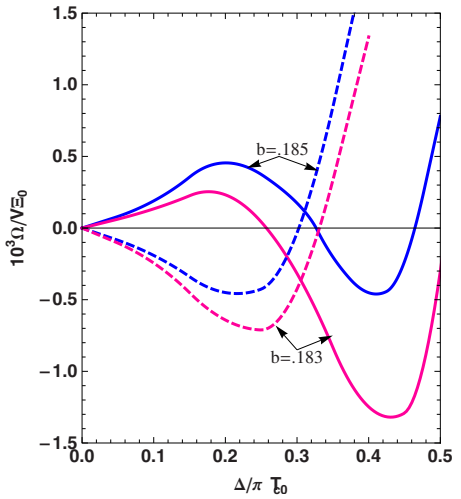


FIG. 5. (Color online) $\Omega$ vs $\bar{\Delta}_{\max}$ (in units of $\Xi_0 V$) for a uniform ($q=0$) SC order parameter (solid curves) and for the corresponding FF modulated order parameter (dashed curves) at various magnetic field values $b$ near the SC transition of an isotropic 3D system at temperature $t=0.02$. The selected material parameters are the same as in Fig. 4. Note the first-order transition from the FF to the uniform SC state at $b \approx 0.185$.

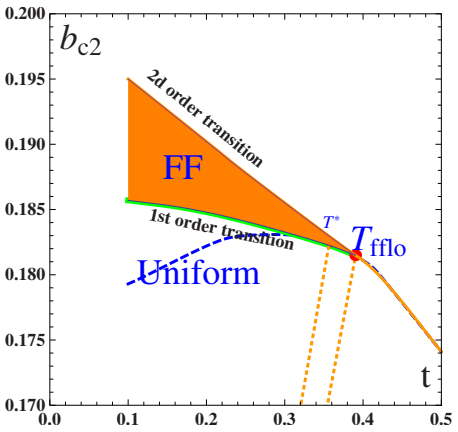


FIG. 6. (Color online) A quantitative $bt$-phase diagram for an isotropic 3D heavy-fermion metal (material parameters are the same as in Fig. 4, characterizing $URu_2Si_2$). The thin (orange) solid line separates the normal and SC phases at second-order phase transitions. Below $T_{fflo}$ the transitions are to a modulated SC state whereas above $T_{fflo}$ the transitions are to a uniform state. The thick (green) solid line corresponds to the first-order phase transition between FF (shaded area) and uniform SC states. The (blue) dashed line is obtained from the usual equation $\alpha(t,b)=0$. The parallel straight (orange) dashed lines, originating from the points $T_{fflo}$ and $T^*$, are determined by the equations $\kappa(t,b)=0$ and $\beta(t,b)=0$, respectively.

within third-order perturbation theory, by $\alpha=\frac{3\beta^2}{16\gamma}>0$) at a critical field $H_{c2}^{(1)}>H_{c2}^{(0)}$.

The correct value of $H_{c2}^{(1)}$ can be determined, however (except for $T\lesssim T_{fflo}$), only by the nonperturbative theory since at the first-order transition $\bar{\Delta}_{\max}^2$ jumps to a relatively large value ($\gtrsim 0.04$). The relative magnitude of $T_{fflo}$ and $T^*$, as well as of $H_{c2}^{(2)}$ and $H_{c2}^{(1)}$, depends on the dimensionality of the FS and will be considered separately for an isotropic 3D and quasi-2D systems in the following sections.

### A. Isotropic 3D system

For a clean isotropic 3D system one has: $T_{fflo}>T^*$, $H_{c2}^{(2)}>H_{c2}^{(1)}$, and within perturbation theory (see Ref. 13) $T=T_{fflo}$ is a tricritical point at the edge of an intermediate nonuniform SC phase, which is separated from the normal state by a second-order transition line and from the uniform (BCS) state by a first-order transition line (see Fig. 6). Just below $T_{fflo}$, where the order parameters for both transition lines are sufficiently small, the corresponding mean-field value, $\Omega_{\min}(q)\sim-\frac{\alpha^2}{2\beta}$, of the GL TP, $\Omega_{pert}/V\Xi_0=\alpha\bar{\Delta}_{\max}^2+\frac{1}{2}\beta\bar{\Delta}_{\max}^4$, has a double-well structure with two local minima at $q=q_{opt}$ and 0. The former minimum has a lower energy at high field whereas the latter becomes energetically favorable at lower field, predicting a weak first-order phase transition from the modulated to the uniform state just below $H_{c2}^{(0)}$, since $\Omega_{\min}(q=0)$ changes much faster with the magnetic field than $\Omega_{\min}(q=q_{opt})$.

At $T\lesssim T^*$, because of the strong variation in $\beta(q)$ around zero (see Fig. 3), the perturbation theory is unstable and the two SC phases can be properly described only within the nonperturbative approach. Thus, considering Eq. (13) for the TP, the general form of $\Omega(\bar{\Delta}_{\max}^2)$ as a function of $\bar{\Delta}_{\max}^2$ is controlled by the argument $\bar{\Delta}_{\max}^2 e^{-u^2}\bar{\Theta}_\nu$, which is always real and positive in the absence of spin splitting, but can become complex for the uniform ($q=0$) state at large spin splitting $g$. Under these circumstances it is easy to show that $\Omega$ has a maximum at small $\bar{\Delta}_{\max}^2$ which is followed by a minimum at larger $\bar{\Delta}_{\max}^2$ (see the solid lines in Fig. 5). Physically, the initial maximum reflects the competition between the increasing spin paramagnetic energy and decreasing SC pair-correlation energy as the number of spin-singlet Cooper pairs is increased. This anomalous feature is "healed" by introducing an FF modulation wave number $q\neq 0$, which restores the usual single minimum structure (shown by the dashed lines in Fig. 5). At high fields the usual single minimum at small $\bar{\Delta}_{\max}^2$ for the modulated state (with $q\neq 0$) corresponds to the equilibrium state.

However, due to its compensation effect, the FF modulation strongly reduces the scale of the SC free energy with respect to its uniform counterpart (compare the dashed curves to the corresponding solid ones in Fig. 5), so that by slightly reducing the field below the second-order normal-to-SC transition, the $q=0$ state becomes energetically more favorable and the system transforms from the nonuniform to a uniform SC state via a first-order phase transition.

The calculated mean-field phase diagram is shown in Fig. 6. The differences between the results predicted by the perturbative and nonperturbative approaches are remarkable. In particular, the line determined from the condition $\kappa=0$, interpreted commonly as an internal SC phase boundary between the modulated (FF) and the uniform SC states, deviates qualitatively from the actual phase transitions line obtained in the present nonperturbative method. The result-

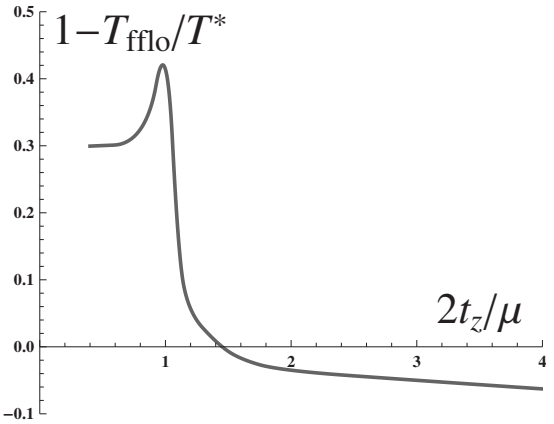


FIG. 7. A plot of $1-T_{fflo}/T^*$ as a function of the dimensionality parameter $2t_z/\mu$, showing the crossover from a three-phase diagram (shown, e.g., in Fig. 6) in the 3D limit ($2t_z/\mu \gg 1$) to a two-phase diagram (shown, e.g., in Fig. 8) in the quasi-2D limit ($2t_z/\mu \ll 1$).

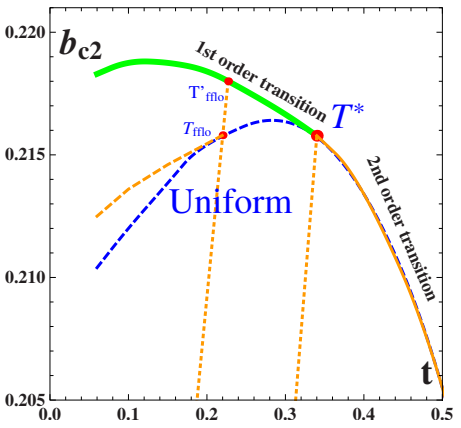


FIG. 8. (Color online) *bt*-phase diagram for a quasi-2D heavy-fermion metal. Notations are the same as in Fig. 7. The material parameters used, $t_z=1.8$, $\bar{g}=1.5$, $\bar{\mu}=30$, are characteristic of $CeCoIn_5$.

ing modulated SC phase is restricted to a very narrow strip below the (second-order) phase transition line to the SC state, which might be difficult to resolve experimentally.

### B. Quasi 2D systems

As indicated in the introduction, the perturbative calculations employed in Ref. 13 predict that the dimensionality characterizing the Fermi surface of the various materials under study plays a crucial role in the fine balance between the tendency of the system toward a uniform SC state via a discontinuous phase transition or toward a modulated (FFLO) phase. The situation can be illustrated by plotting the ratio of $T_{fflo}$ to $T^*$ as a function of the dimensionality parameter, $2t_z/\mu$, which is the maximal electron energy, $\varepsilon^{(q2D)}_{\mathbf{k}=0,k_z=\pi/c}$, perpendicular to the easy conducting plane, measured relative to the Fermi energy (see Fig. 7). Consistently with our previous result, based on a different quasi-2D model,[13] it is found here that $T_{fflo}$ is suppressed more strongly than $T^*$ by decreasing $2t_z/\mu$ toward the 2D limit, so that below some critical value of $2t_z/\mu(\simeq 1.4)$ there is a changeover to first-order SC phase transitions. We have found that this critical value increases with increasing Fermi energy when all other parameters, except for $t_z$, remain fixed.

The sharp feature seen in Fig. 7 at $t_z=\mu/2$, i.e., where the FS touches the BZ boundary perpendicular to the $z$ axis, arises from the sharp minimum characterizing the scaling factor $\eta(t_z)$ at $t_z=\mu/2$ [see Eq. (15)]. The origin of this minimum is in the sharp maximum of $H_{c20}(t_z)$ at $t_z=\mu/2$ for which the condition $\bar{\xi}_{\mathbf{k},k_z}\simeq 0$ in the denominator of the GF, Eq. (14), at $t=0$ corresponds to a sharp resonance, where open channels with small cyclotron energy [i.e., with $k\to 0$ and large $k_z(\approx \pi/c)$] near the FS suppress the diamagnetic effect [i.e., causing $w(x_\nu)\to 1$].

Considering the quasi-2D region $2t_z/\mu \ll 1$, where $T^* > T_{fflo}$, the question arises as to whether a modulated (FF) phase can be stabilized above the nominal transition line, determined by $\kappa=\frac{\partial^2}{\partial q^2}\alpha(q=0)=0$ (dotted line in Fig. 8), as proposed by several authors,[14,15] following predictions based on perturbative approach.[9–11] The failures of the perturbative approaches, discussed in the previous section, entails a careful re-examination of this prediction within the framework of the present nonperturbative approach. Thus, investigating the TP given by Eq. (13) in the quasi-2D regime in a manner similar to that done for the isotropic 3D case presented in Fig. 5, it is found that the uniform SC phase, created discontinuously at the first-order transition line below $T^*$, remains stable with respect to formation of a modulated FF state in the entire phase-diagram region below $T^*$ (see Fig. 8).

This finding is in accord with the very narrow region, found in the phase diagram shown in Fig. 6, for a modulated (FF) state in the most favorable situation of an isotropic 3D superconductor. In the present, unfavorable case, of a quasi-2D system the competition between the already stable minimum of the TP for the uniform SC state at finite $\bar{\Delta}^2_{\max}$ and the metastable minimum for the modulated state at small $\bar{\Delta}^2_{\max}$ under decreasing field (or temperature) below the first-order transition line (thick solid line in Fig. 8) is a lost battle for the modulated state due to its smaller scale of SC condensation energy. Similar conclusion is expected to hold also for a multimode modulation, such as in the LO (Ref. 7) state, since the price paid in terms of electron-pair kinetic energy for the creation of any modulated state (FF or LO) with the same wave number $q$ is the same. Consequently, the corresponding change in the SC condensation energy (arising from compensation of the Zeeman spin-splitting energy) cannot be drastically different for the different modulated states, so that the tendency of the system to stabilize in any modulated state cannot compete with its much stronger tendency to transform into a uniform state via a first-order transition.

## IV. DISCUSSION AND COMPARISON WITH EXPERIMENT

Among the many candidate materials proposed over the years for observing strong paramagnetic effects on their SC phase transitions, the heavy-fermion superconductor $CeCoIn_5$ is the most extensively studied. It has a layered

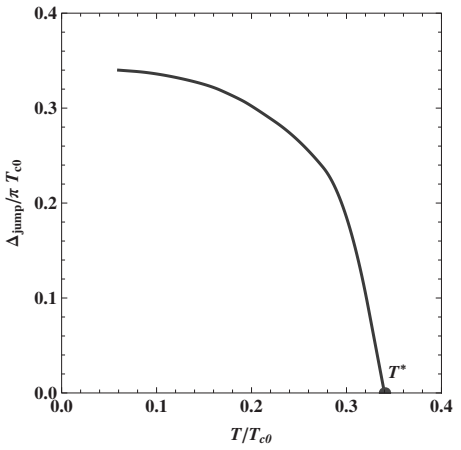


FIG. 9. Temperature dependence of the jump, $\bar{\Delta}_{jump}$, of the order parameter at the first-order transition, showing rapid variation near the changeover point $t=t^*=0.34$. Parameters are the same as in Fig. 8.

crystal structure and moderate quasi-2D electronic band structure,[2] which favors a changeover to first-order SC phase transitions directly from the normal state. Such a changeover has been reported in various experimental probes, including specific-heat,[14] magnetization,[16] and NMR (Ref. 15) measurements. The main features of the high-fields low-temperatures corner of its phase diagram for a magnetic field parallel to the *c* axis (see, e.g., Refs. 14 and 15) is quantitatively accounted for by Fig. 8. The possibility of a modulated FF or LO state, discussed extensively in these papers, is inconsistent, however, with our finding. Our nonperturbative calculations of the SC free energy show clearly that for a quasi-2D system, where a first-order phase transition takes place from the normal to a *uniform* SC phase, a modulated (FF) SC phase is energetically less favorable than the uniform phase. This conclusion seems to agree with very recent neutron-scattering experiment,[23] showing strong evidence for a magnetic order as origin of the observed modulation in the SC order parameter, rather than FF or LO modulation.

An important measurable quantity is the jump, $\bar{\Delta}_{jump}(t)$, of the SC order parameter at the first-order transition, which exhibits a typical temperature dependence as shown in Fig. 9 for parameters characterizing $CeCoIn_5$. The development of the mean-field order parameter, $\bar{\Delta}_{\max}$, with the magnetic field at and below the SC transition for a given temperature is determined by the minima of the calculated SC TP as a function of the order parameter for different magnetic field values, as shown in Fig. 10(a). At a field slightly above $b_{c2}(t)$ the TP develops a shallow, metastable minimum, which becomes degenerate with the normal-state minimum at the finite value of the order parameter, $\bar{\Delta}_{\max}=\bar{\Delta}_{jump}$ [$\sim$0.34 for $t=0.1$, see Fig. 10(a)] determining $b_{c2}(t)$. Except for the high-temperature region near the critical point $t=t^*$, where $\bar{\Delta}_{jump}$ sharply increases from zero (see Fig. 9), the mean-field value $\bar{\Delta}_{\max}(b)$ increases weakly with the decreasing magnetic field below $b_{c2}(t)$ up to a value, at zero field, which is approximately $2\bar{\Delta}_{jump}$ [see Figs. 10(a) and 10(b)]. This behavior is different from that characterizing the discontinuous phase transition in a 3D system, discussed in Sec. III A, where the order parameter jump is approximately twice smaller than its variation below the first-order transition.

It should be noted that this mean-field picture is expected to change significantly by thermal (or/and quantum) fluctuations due to the very small activation barrier separating the two degenerate minima at the first-order transition shown in Fig. 10(a).

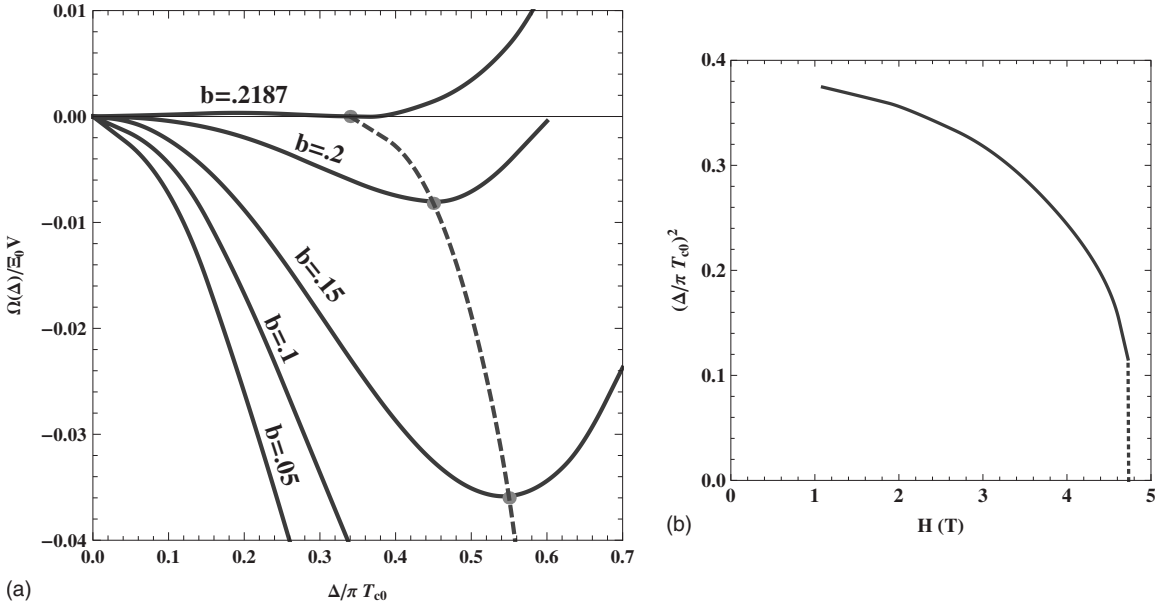


FIG. 10. (a) SC free energy as a function of order parameter for different field values below the first-order SC phase transition at temperature $t=0.1$. Dashed line is the locus of minima determining the mean-field values, $\bar{\Delta}_{\max}(b)$. Parameters are the same as in Fig. 8. (b) Magnetic field dependence of $\bar{\Delta}^2_{\max}$ (in the mean-field approximation), as determined from the TP shown in panel (a).

Our nonperturbative approach can be applied to the calculation of magnetization near the first-order SC transition, and compared with experimental data, reported, e.g., in Ref. 16. Using Eq. (13) the SC contribution to the magnetization is readily calculated (since the explicit dependence on magnetic field originates only in the effective Green's function), yielding

$$\frac{M}{V} = -\frac{\partial}{\partial H}\frac{\Omega}{V} = \frac{1}{H_{c20}}\frac{a_x}{\sqrt{2\pi}}\frac{k_B T_{c0}}{\xi^3} t\,\mathrm{Re}\sum_{\nu>0}\left\langle \int \frac{d^3k}{(2\pi)^3}\frac{e^{-u^2}\bar{\Delta}_{\max}^2 \frac{\partial}{\partial b}[\Phi_\nu(\mathbf{k},k_z|g,q)\Phi_\nu^*(\mathbf{k},k_z|-g,-q)]}{1+e^{-u^2}\bar{\Delta}_{\max}^2 e^{-u^2}\bar{\Phi}_\nu(\mathbf{k},k_z|g,q)\bar{\Phi}_\nu^*(\mathbf{k},k_z|-g,-q)}\right\rangle_u . \tag{20}$$

To compare with the experimental data we have added an empirical normal-state contribution by extrapolating the observed field-dependent magnetization above the transition to the SC region. The result is shown in Fig. 11, together with the experimental data. The good quantitative agreement is particularly remarkable in light of the fact that no adjustable parameter, other than the absolute scale of the magnetization, has been assumed in the fitting.

Finally, de Haas–van Alphen (dHvA) oscillation has been observed both in the normal and SC mixed states in $CeCoIn_5$,[24] showing a very sharp additional damping at the SC transition for magnetic field direction perpendicular to the easy conducting layers, which seems to be consistent with the occurrence of a first-order SC phase transition.

Assigning the sharp rise, $\delta T_D \simeq 0.08$ K, of the Dingle temperature observed in the dHvA measurements[24] to the discontinuous jump, $\delta\Delta$, of the SC order parameter at the first-order transition, $\delta T_D$ may be calculated by exploiting the random vortex lattice model[19] with the formula

$$\delta T_D = T_{c0}\frac{\sqrt{\pi}}{2}(\delta\bar{\Delta})^2\frac{\pi k_B T_{c0}}{\hbar\omega_{c2}}\sqrt{\frac{H_{c2}}{F}},$$

where $F$ is the relevant dHvA frequency. Using the experimental values: $g=14.8$, $F=5000$ T, $T_{c0}=2.3$ K, and $H_{c2}=4.8$ T, and the calculated value of the jump $\delta\bar{\Delta}\simeq 0.34$, we arrive at: $\delta T_D^{(cal)} \approx 0.12$ K, which agrees rather well with the experimental value of $\delta T_D \simeq .08$ K.

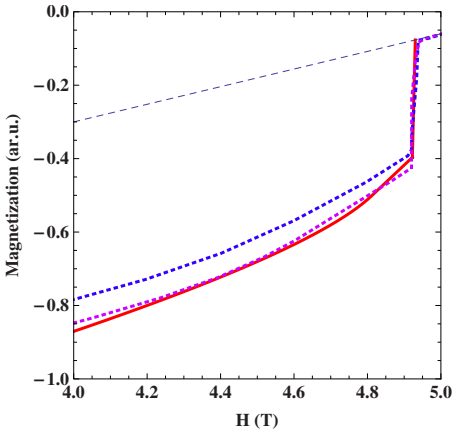


FIG. 11. (Color online) Experimental (Ref. 16) (violet and blue dotted lines for up and down sweeps, respectively) and theoretical (solid red line) magnetization as functions of the magnetic field at $T=30$ mK in $CeCoIn_5$. The normal-state contribution below $H_{c2}$ was obtained by a linear extrapolation of the measured magnetization in the normal state (dashed line).

Similarly, using our nonperturbative approach, we have shown in a separate communication[25] that the dHvA effect observed in the mixed SC state of $URu_2Si_2$ (Ref. 3) provides a clear experimental evidence for the predicted double-stage nature of the low-temperature high-field SC transition in 3D superconductors, which is smeared by significant SC fluctuations effect. This finding is basically consistent with the interpretation of a first-order phase transition given in Ref. 17 to the single (smeared) steplike structure observed in the thermal transport data of this material, which seems to hide the continuous phase transition within the tail of the nearby first-order transition. The double-stage structure can be resolved experimentally only by probes, such as the dHvA measurements reported in Ref. 3, sufficiently sensitive to the variation in the order parameter in the narrow transition region.

We note that the unusual sign of the observed jump in the thermal conductivity, which could be due to some peculiar quasiparticle scattering mechanism,[26] is irrelevant to our main argument, which associates this jump, irrespective of its direction, to the jump of the SC order parameter at the predicted first-order transition.

## V. CONCLUSION

In the present paper we have derived a nonperturbative expression for the SC thermodynamic potential of a strongly type-II superconductor in the presence of strong Pauli paramagnetic effect and have determined the corresponding $H$-$T$ phase diagrams for prototype 3D and quasi-2D heavy-fermion compounds. It is found that for quasi-2D heavy-fermion metals, such as $CeCoIn_5$, at high magnetic fields oriented perpendicular to the highly conducting planes, the effect of the Fulde-Ferrel (FF) (or Larkin-Ovchinnikov) modulation is too weak to prevent a first-order phase transition from the normal to the uniform SC state. No modulated FF phase can be, therefore, stabilized at fields below $H_{c2}$ in this kind of materials. The calculated thermodynamic potential yields good quantitative agreement with the experimentally derived phase diagram and measured low-temperature magnetization near $H_{c2}$ in $CeCoIn_5$. For 3D heavy-fermion metals, such as $URu_2Si_2$, the FF modulation stabilizes, under

a decreasing magnetic field, a nonuniform SC state via a second-order phase transition from the normal state. However, at a slightly lower field the modulated phase becomes unstable, transforming to a uniform SC state via a first-order transition. The sharp onset of the SC order parameter calculated for this double-stage scenario of the SC transition, including fluctuation effect, is found to be in good agreement with dHvA results in the SC state of $URu_2Si_2$.

## ACKNOWLEDGMENTS

We thank J. Wosnitza for valuable discussions. This research was supported by the Israel Science Foundation under Grant No. 425/07, by Posnansky Research fund in superconductivity, and by EuroMagNET under the EU (Contract No. RII3-CT-2004-506239).

## APPENDIX A

Starting from the standard expression

$$G_{0\uparrow\downarrow}(\mathbf{r}_1,\mathbf{r}_2,\omega_\nu)=\frac{1}{2\pi a_H^2}\int\frac{dk_z}{2\pi}e^{ik_z(z_2-z_1)}\sum_n\frac{e^{-\rho^2/4}L_n(\rho^2/2)}{\mu-\varepsilon_{nk_z}+i\omega_\nu},$$

where $L_n(\rho^2/2)$ is the Laguerre polynomial of the order $n$ and $\varepsilon_{nk_z}/\hbar\omega_c=n+\tilde{\varepsilon}_z$, one can make use of the integral representation, $\pm i[n_F-n-\tilde{\varepsilon}_z+i\varpi_\nu]^{-1}=\int_0^\infty d\tau e^{\pm i\tau[n_F-n-\tilde{\varepsilon}_z+i\varpi_\nu]}$, and apply the well-known identity, $\Sigma_{n=0}^\infty z^n L_n(t)=(1-z)^{-1}\exp(\frac{tz}{z-1})$ with $z=e^{\pm i\tau}$ and $t=\rho^2/2$, for the summation over LLs, to obtain the expression given by Eq. (4).

## APPENDIX B

For a positive Matsubara frequency the general term of the order-parameter expansion can be written as

$$\Omega_{2n}(\varpi_\nu>0)=\frac{k_BT}{n}\left(\frac{m^\star a_H^3}{2\pi\hbar^2 a_H}\right)^{2n}\frac{2\pi}{\sqrt{3}a_x^2}\Delta_0^{2n}\sum_{\nu>0}\int d^2\mathbf{R}dZ\int_0^\infty\prod d\tau_l e^{-\varpi_\nu\sum_l\tau_l+in_F\sum_l(-1)^l\tau_l-ig\sum_l\tau_l}I_\tau([\tau])I_q([\tau]),$$

$$I_q([\tau])=\int\prod\frac{dk_{l,z}}{2\pi}\frac{dk_z}{2\pi}d\rho_{z,l,l+1}e^{ik_z\Sigma\boldsymbol{\rho}_{z,l,l+1}-i\sum_l(-1)^l\tau_l x_l^2+iq/2\sum_l(-1)^l\rho_{z,l,l+1}+i\sum_l(-1)^l k_l\rho_{z,l,l+1}},$$

$$I_\tau([\tau])=\int\frac{d^2k}{(2\pi)^2}\prod d^2\rho_{l,l+1}(1-\xi_l)^{-1}\exp\left(-\frac{\rho_{l,l+1}^2\xi_l}{2(1-\xi_l)}\right)e^{i\mathbf{k}\Sigma\rho_{l,l+1}-1/2\Sigma\rho_{l,l+1}^2},$$

where $\xi_l=e^{-i(-1)^l\tau_l}$, $x_l^2=\hbar^2k_{l,z}^2/2m\hbar\omega_c$ and

$$\rho_{z,l,l+1}=z_{l+1}-z_l,\quad Z=\frac{1}{2n}\sum z_l,$$

$$\boldsymbol{\rho}_{l,l+1}=\boldsymbol{r}_{l+1}-\boldsymbol{r}_l,\quad \boldsymbol{R}=\frac{1}{2n}\sum\boldsymbol{r}_l$$

are the relative and center of mass coordinates. We have also used the identities: $\exp-iq\Sigma_l(-1)^l z_l=ei\frac{q}{2}\Sigma_l(-1)^l\rho_{z,l,l+1}$ and

$$\prod dz_l=\int\frac{dk_z}{2\pi}e^{ik_z\Sigma\rho_{z,l,l+1}}\prod dZd\rho_{z,l,l+1},$$

$$\prod d^2\boldsymbol{r}_\mathbf{l}=\int\frac{d^2k}{(2\pi)^2}e^{i\mathbf{k}\Sigma\boldsymbol{\rho}_{l,l+1}}d^2\mathbf{R}d^2\rho_{l,l+1}.$$

Let us consider $I_q([\tau])$. Performing first the integrations over relative coordinates, $\rho_{z,l,l+1}$, one obtains the momentum conservations laws which can be used for further integrations over $k_{z,l}$. The resulting expression

$$I_q([\tau])=\int\frac{dk_z}{(2\pi)^2}e^{-i/2\Sigma(-1)^l\tau_l[k_z+(-1)^lq/2]^2}$$

is factorized with respect to $\tau_l$.

The integrals over relative coordinates in $I_\tau([\tau])$ are of the Gaussian type which are estimated as

$$\int d^2\rho_{l,l+1}e^{i\mathbf{k}\rho_{l,l+1}}e^{-1/2\rho_{l,l+1}^2}(1-\xi_l)^{-1}\exp\left(-\frac{\rho_{l,l+1}^2\xi_l}{2(1-\xi_l)}\right)$$
$$=2\pi e^{-1/2(1-\xi_l)\mathbf{k}^2},$$

leading again to factorized representation

$$I_\tau([\tau])=(2\pi)^{2n}\int\frac{d^2k}{2\pi}\prod e^{-1/2(1-\xi_l)\mathbf{k}^2}.$$

Collecting all factors depending on $\tau_l$ in $\Omega_{2n}$ one arrives at the desired formula, Eq. (6) for $\varpi_\nu>0$. The contribution for negative $\nu<0$ can simply obtained by replacement $\tau_l\to-\tau_l$ which produce the complex conjugate expression to $\Omega_{2n}(\varpi_\nu>0)$.

[1] A. M. Clogston, Phys. Rev. Lett. **9**, 266 (1962); B. S. Chandrasekhar, Appl. Phys. Lett. **1**, 7 (1962).
[2] R. Settai, H. Shishido, S. Ikeda, Y. Murakawa, M. Nakashima, D. Aoki, Y. Haga, H. Harima, and Y. Onuki, J. Phys.: Condens. Matter **13**, L627 (2001).
[3] H. Ohkuni, Y. Inada, Y. Tokiwa, K. Sakurai, R. Settai, T. Honma, Y. Haga, E. Yamamoto, Y. Onuki, H. Yamagami, S. Takahashi, and T. Yanagisawa, Philos. Mag. B **79**, 1045 (1999).
[4] G. Sarma, J. Phys. Chem. Solids **24**, 1029 (1963).
[5] K. Maki and T. Tsuneto, Prog. Theor. Phys. **31**, 945 (1964).
[6] P. Fulde and R. A. Ferrell, Phys. Rev. **135**, A550 (1964).
[7] A. I. Larkin and Yu. N. Ovchinnikov, Zh. Eksp. Teor. Fiz. **47**, 1136 (1964) [Sov. Phys. JETP **20**, 762 (1965)].
[8] L. W. Gruenberg and L. Gunther, Phys. Rev. Lett. **16**, 996 (1966).
[9] D. F. Agterberg and K. Yang, J. Phys.: Condens. Matter **13**, 9259 (2001).
[10] M. Houzet and A. Buzdin, Phys. Rev. B **63**, 184521 (2001).
[11] H. Adachi and R. Ikeda, Phys. Rev. B **68**, 184510 (2003).
[12] M. Houzet and V. P. Mineev, Phys. Rev. B **74**, 144522 (2006).
[13] T. Maniv and V. Zhuravlev, Phys. Rev. B **77**, 134511 (2008).
[14] A. Bianchi, R. Movshovich, N. Oeschler, P. Gegenwart, F. Steglich, J. D. Thompson, P. G. Pagliuso, and J. L. Sarrao, Phys. Rev. Lett. **89**, 137002 (2002); A. Bianchi, R. Movshovich, C. Capan, P. G. Pagliuso, and J. L. Sarrao, *ibid.* **91**, 187004 (2003).
[15] K. Kumagai, M. Saitoh, T. Oyaizu, Y. Furukawa, S. Takashima, M. Nohara, H. Takagi, and Y. Matsuda, Phys. Rev. Lett. **97**, 227002 (2006).
[16] X. Gratens, L Mendonca Ferreira, Y. Kopelevich, N. F. Oliveira Jr., P. G. Pagliuso, R. Movshovich, R. R. Urbano, J. L. Sarrao, and J. D. Thompson, arXiv:cond-mat/0608722v1 (unpublished).
[17] Y. Kasahara, T. Iwasawa, H. Shishido, T. Shibauchi, K. Behnia, Y. Haga, T. D. Matsuda, Y. Onuki, M. Sigrist, and Y. Matsuda, Phys. Rev. Lett. **99**, 116402 (2007).
[18] V. N. Zhuravlev, T. Maniv, I. D. Vagner, and P. Wyder, Phys. Rev. B **56**, 14693 (1997).
[19] T. Maniv, V. Zhuravlev, I. Vagner, and P. Wyder, Rev. Mod. Phys. **73**, 867 (2001).
[20] M. Rasolt and Z. Tesanovic, Rev. Mod. Phys. **64**, 709 (1992).
[21] A. A. Abrikosov, L. P. Gorkov, and I. E. Dzyaloshinski, *Methods of Quantum Field Theory in Statistical Physics* (Dover, New York, 1975).
[22] E. Helfand and N. R. Werthamer, Phys. Rev. **147**, 288 (1966); N. R. Werthamer, E. Helfand, and P. C. Hohenberg, *ibid.* **147**, 295 (1966).
[23] M. Kenzelmann, Th. Strassle, C. Niedermayer, M. Sigrist, B. Padmanabhan, M. Zolliker, A. D. Bianchi, R. Movshovich, E. D. Bauer, J. L. Sarrao, and J. D. Thompson, Science **321**, 1652 (2008).
[24] R. Settai, H. Shishido, S. Ikeda, M. Nakashima, D. Aoki, Y. Haga, H. Harima, and Y. Ōnuki, Physica B (Amsterdam) **312-313**, 123 (2002).
[25] V. Zhuravlev and T. Maniv, arXiv:0902.0438 (unpublished).
[26] H. Adachi and M. Sigrist, J. Phys. Soc. Jpn. **77**, 053704 (2008).